New Insights into the Thermal Stability of the Smectic C Phase

ARTICLE *in* THE JOURNAL OF PHYSICAL CHEMISTRY B · MARCH 2014

Impact Factor: 3.3 · DOI: 10.1021/jp5011605 · Source: PubMed

4 AUTHORS, INCLUDING:

Francois Porzio
Université de Sherbrooke
10 PUBLICATIONS **21** CITATIONS
SEE PROFILE

Etienne Levert
Siboire Microbrewery
6 PUBLICATIONS **15** CITATIONS
SEE PROFILE

Armand Soldera
Université de Sherbrooke
95 PUBLICATIONS **896** CITATIONS
SEE PROFILE

THE JOURNAL OF PHYSICAL CHEMISTRY B

Article

pubs.acs.org/JPCB

New Insights into the Thermal Stability of the Smectic C Phase

François Porzio, Etienne Levert, Richard Vadnais, and Armand Soldera*

Centre Québécois des Matériaux Fonctionnels (CQMF), Département de Chimie, Université de Sherbrooke, Sherbrooke (Québec) J1K 2R1, Canada

Supporting Information

ABSTRACT: Subtle differences in the molecular structure of mesogens can lead to very different experimental polymorphisms. The smectic C (SmC) phase can actually be exhibited by one isomer and not the other, or the range of temperature can be completely different. Unveiling the deep connection between atomic structure and the very existence of the SmC phase will lead to the design of new performing liquid crystalline materials for ferroelectric or nonlinear optical applications. Our approach is based on running molecular dynamics simulation from an initial SmC arrangement of molecules. When the temperature is increased, the molecules automatically adjust in a more favorable organization. Such modification in the imposed initial self-assembly is governed by values of the nonbonded energies. Thanks to the combined use of simulation and experimental phase diagrams, we have unveiled part of the deep connection between atomic structure and the very existence of the SmC phase. The actual display of the SmC mesophase stems from a subtle balance between short-range interactions, which reveal arrangement of molecules within a smectic layer, and long-range interactions, which disclose organization of layers.

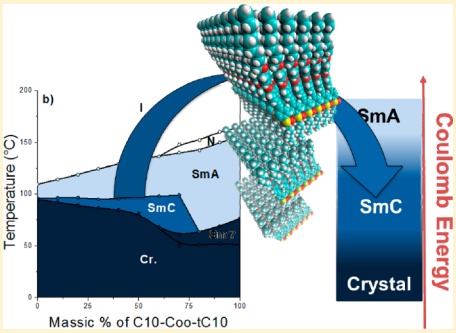

INTRODUCTION

Small changes in the architecture of a molecule can impart drastic modifications of properties to the ensuing material. This link between microscopic and macroscopic scales among interacting systems is far from clear. Statistical physics gives the theoretical tools to study it, and molecular simulation provides the means to apply them to complex systems, such as liquid crystals (LC). This particular state of matter is in fact particularly interesting in striving to disclose the subtle link between these two scales. The great variety of mesogens, i.e. molecules which exhibit LC phases in their polymorphism, has made possible the establishment of relationships between molecular architecture and occurrence of specific mesophases. Early works formulated basic structure−property relationships on the account of the overall geometry[1] and the presence of outboard or in-core dipoles.[2] These empirical rules offer general guidelines for the synthesis of mesogens.[3] They were of particular interest to get mesogens displaying the largest domain of thermal stability of the smectic C (SmC) phase for ferroelectric liquid crystal applications[4] or nonlinear optical applications.[5−7] This mesophase is generally recognized to be fostered by the increase in the lengthening of the rigid core or the lateral alkyl chains.[8] Thanks to the development of computer resources and efficiency of codes, molecular simulation became a valuable tool to capture these effects.[9] Moreover, it can give insight into the arrangement of molecules within this mesophase which is not fully understood[9] and for which no comprehensive theory actually exists.[10]

A very interesting review on molecular simulation of LC was made by Wilson in 2007.[9] To better address long-range interactions that mainly govern formation of mesophases,[11] coarse-grained methods have been identified to be mostly appropriate. Recent achievements at this level of simulation are for example the study of the formation of membrane possessing a nematic order,[12] LC nanoclusters,[13] or the depiction of nematic−isotropic liquid-phase transition.[14] However, such an approach is not suited for revealing small molecular changes that account for differences in the LC polymorphism. Full atomistic simulation provides finer details at the expense of depiction of long-range interactions. Nevertheless, Berardi et al. used this technique to disclose the nematic-to-isotropic transition and correctly reproduced the experimental odd−even effect.[15]

The cornerstone of our study is the use of structural isomers to reveal their different liquid crystalline polymorphisms by atomistic simulation. More specifically, the focus is on the thermal stability of the SmC phase of these isomers. From a molecular simulation viewpoint, the use of isomers is of particular interest because they share the same force field parameters. Any changes observed in the computed properties are then attributed to differences in molecular characteristics only.[16,17] Molecular simulation of these two isomers can thus account for difference in their liquid crystalline polymorphism without exploring a very large portion of phase space. We thus focused our studies on two series of isomeric calamitic mesogens shown in Chart 1. Differences in these compounds lie in the direction of the in-core dipole (isomerism) and in the outboard dipole (sulfinic or carboxylic esters). Variations of

Received: February 1, 2014
Revised: March 17, 2014
Published: March 17, 2014

   dx.doi.org/10.1021/jp5011605 | J. Phys. Chem. B 2014, 118, 4037−4043

Chart 1. Molecular Structures and Nomenclature of the Two Series of Liquid Crystals, Where X Is a Carbon or Sulfur Atom

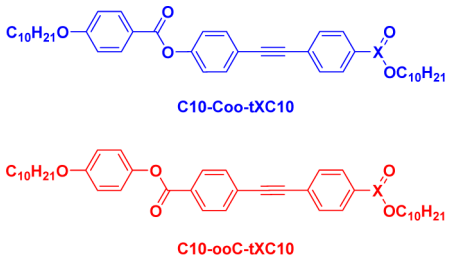

these molecular characteristics greatly impact the very existence of the SmC phase (Figure 1). A nomenclature is introduced to

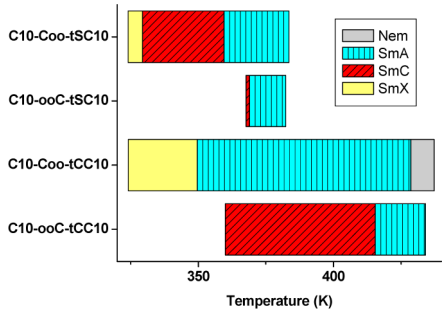

Figure 1. Experimental polymorphism of the S-series and C-series with alkyl terminal chains containing 10 carbon atoms. SmX is uncharacterized smectic phase.

identify the studied mesogens (Chart 1): the length of the alkane chain is symbolized by C10 (10 carbon atoms); the orientation of the in-core dipole over the tolane core (symbolized by t) is represented by the letters Coo-t or ooC-t; and finally the nature of the outboard dipole is displayed by a letter, X = C for ester or X = S for sulfinic ester.

In previous studies, we reported full-atomistic molecular dynamics (MD) simulations of ester molecules (X = C in Chart 1), the actual C-series.[18] The effect of the in-core dipole orientation as well as the chain length have been analyzed according to the nonbonded potential energies.[18] It has been argued that a strong (more negative) long-range Coulomb potential, as has been observed for C10-ooC-tCC10 (Chart 1), is concomitant with the occurrence of the SmC phase. Is this conclusion supported by other mesogens? To answer this question, the procedure we used to simulate mesogens of the C-series is applied to the other series of isomers, the S-series (Chart 1), whose difference with its homologue of the C-series lies on the outboard dipoles. The noteworthy point is that they exhibit very different liquid crystal polymorphisms (Figure 1). To investigate the molecular reasons for this difference, MD simulations and experiments are carried out in a complementary way.

SIMULATION DETAILS

The procedure to generate the liquid crystalline phase is detailed in a previous article.[18] The approach is summarized herein. One configuration consists of an array of 144 molecules distributed along 3 layers embedded in a cell with periodic boundary conditions. To better represent the phase space, four different starting simulation cells have been constructed for each of the four studied molecules (Chart 1). Each cell thus corresponds to one configuration where molecules are in different conformations. The very purpose of the suggested approach is to build cells with molecules in the SmC arrangement. In Figure 2a, an initial configuration is shown.

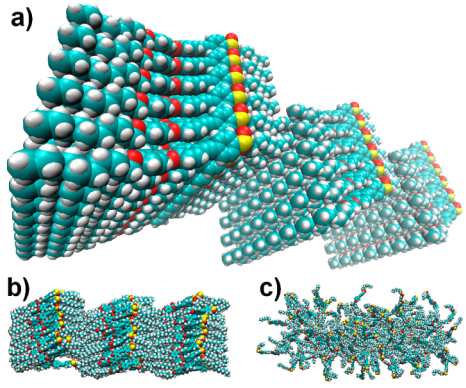

Figure 2. Atomistic representation[19] of (a) an initial configuration, (b) the cell at 310 K, and (c) the cell at 650 K (the corresponding radial distribution is displayed in Figure S1 of the Supporting Information). Images through the periodic boundary conditions are not displayed.

The volume of the cell is 3 × 4 × 13 nm^3. For clarity, images from periodic boundary conditions are not displayed. The unit cell corresponds to 144 molecules. When the temperature is increased, this initial packing is disorganized (Figure 2b) to become isotropic (Figure 2c, and Figure S1 of the Supporting Information for the radial distribution function). There are several benefits in such an approach. First, we circumvent the great difficulties in reaching liquid crystalline order from the liquid phase because of the complexity in exploring the configurational space. Second, similar arrangement for the different systems allows direct comparison. In fact, each cell undergoes the same heating protocol. Any difference in energy of the studied isomers is thus attributed to variations in the initial SmC organization of molecules.

To characterize interactions, the optimized potential for liquid simulations (OPLS) force field was selected.[20] There are two main reasons we have considered this force field. It has been specifically built up to characterize nonbonded interactions among organic molecules in the liquid phase.[20] Such interactions are known to dominate the mesophase behavior.[8] A force field actually consists of equations that tend to mimic specific interactions and parameters stemming from the fit of these equations to ab initio calculations or experimental data. A protocol exists to modify the OPLS force field parameters when specific interactions are missing, as is the case for sulfinic esters.[20] This well-established procedure is the second main reason we chose the OPLS force field. The nonbonded and bonded terms that characterize this force field are briefly described.

The nonbonded potential energy is split into two terms: Lennard-Jones and Coulomb potential. The van der Waals (vdW) interaction is represented by the Lennard-Jones 12−6 potential, eq 1, that characterizes nonpermanent dipole moments.[21]

$$E_{LJ} = \sum_{i>j} \left[4\varepsilon_{ij} \left(\left(\frac{\sigma_{ij}}{ri_j} \right)^{12} - \left(\frac{\sigma_{ij}}{ri_j} \right)^{6} \right) \right] \quad (1)$$

dx.doi.org/10.1021/jp5011605 | J. Phys. Chem. B 2014, 118, 4037−4043

where $\varepsilon_{ij} = (\varepsilon_{ii}\cdot\varepsilon_{jj})^{1/2}$ and $\sigma_{ij} = (\sigma_{ii}\cdot\sigma_{jj})^{1/2}$; ε_{ii}, σ_{ii}, and r_{ij} stand for the depth of the potential well for the interaction between two atoms i, the distance at which the energy between two atoms i is zero, and the distance between atoms i and j, respectively.

The Coulomb interaction, eq 2, deals with the partial charges that are carried by atoms and stem from differences in electronegativity that characterized nonzero local electrical moments.[21]

$$E_C = \sum_{i>j} \frac{q_i\cdot q_j}{\varepsilon\cdot r_{ij}} \tag{2}$$

where $\varepsilon = 4\pi\varepsilon_0$; q_i, ε_0, and r_{ij} stand for the partial charge of atom i, the permittivity of free space, and the distance between atoms i and j, respectively. For sake of efficiency, Coulomb interactions are treated within the Ewald summation method, which replaces the slowly convergent sum of eq 2 by two quickly convergent sums, in direct and reciprocal space separately.[22,23]

The bonded terms consist of a bond-stretching term, an angle-bending term, and a torsional term. Bond-stretching and angle-bending terms are both characterized by a quadratic equation $E = k(q - q_0)^2$, where q stands for the bond or the angle between two atoms and the subscript 0 corresponds to the equilibrium value. The torsional term is shown in eq 3.

$$E_C = \frac{1}{2}\sum_{n=1}^{4} C_n[1 + (-1)^{n+1}\cos(n\phi)] \tag{3}$$

where C_n and ϕ stand for the coefficients in the Fourier series and the dihedral angle value, respectively.

Some OPLS force field parameters that are required to describe interactions involving sulfinic ester molecules were missing (Figure 3). Bonding elongation and bending terms

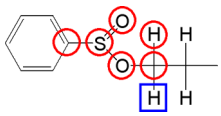

Figure 3. Identification of the six atom types (red circles) missing from the original OPLS force field. The seventh atom (blue square) is also included in this neutral group of charges.

were computed using the methodology established by Jorgensen et al.[20] The ab initio Hartree−Fock method with the 6-31G(d) basis set was chosen. Calculations were run within the Gausian09 software.[24] However, to handle the dihedral contribution, a specific procedure was carried out. Energy curves stemming from ab initio calculations consist of a combination of bonded (eq 3) and nonbonded interactions (eqs 1 and 2). This latter contribution was computed using the BOSS software.[25] The resulting curve was then subtracted from the original curve computed by the ab initio method to retrieve parameters associated with the bonded torsional term only (eq 3). The ε_{ii} and σ_{ii} nonbonded terms already exist in the OPLS force field because they mainly depend on hybridization. Conversely, the partial charges for the seven atoms identified in Figure 3 were missing. They were thus computed using the electrostatic potential scheme in the Gaussian09 environment.[20] The actual charges were adjusted to maintain the electroneutrality of this group of atoms and to guarantee consistency with other charges of the force field. Computed parameters are shown in the Supporting Information (Tables S1−S4).

Once all the force field parameters had been retrieved, MD simulations were performed within the GROMACS environment.[26−30] Newton's equations of motion were integrated using the Verlet leapfrog algorithm, allowing an integration step of 1 fs.[31,32] Simulations were run in the *NPT* ensemble, i.e. the number of atoms, the pressure, and the temperature, are kept constant. To control temperature and pressure, Nosé−Hoover[33,34] and Parrinello−Rahman[35] algorithms were employed, respectively. The simulation cells of the C-series and S-series were heated from 300 and 260 K to 650 K, respectively. At each temperature, the duration of a MD simulation is 5 ns. The simulation cell at the end of the first nanosecond of simulation was used as the starting configuration at the next temperature MD run. Cells are then saved every picosecond during the last nanosecond of the trajectory. Each energy contribution is thus averaged over 1000 frames. A second average over the four configurations of each system was subsequently done.

EXPERIMENT

The synthesis of the mesogens of the C-series and the S-series were reported in the works of Vadnais et al.[36] and Levert et al.,[37] respectively. Preparation and characterization of the binary mixtures to generate binary phase diagrams were achieved using a previously published procedure.[37] The mixtures were prepared by measuring precise volumes of diluted solutions of the mesogens in dichloromethane to obtain the desired weight percentage of each of the mesogens. The solutions were then evaporated under reduced pressure and kept under vacuum for 12 h to get rid of the dichloromethane. The polymorphism of the binary mixtures was then characterized by differential scanning calorimetry and polarized optical microscopy.

RESULTS AND DISCUSSION

The approach we established is based on carrying out MD simulations by gradually increasing the temperature from an initial SmC arrangement of molecules. If such an arrangement is not favorable for the studied mesogens, molecular changes will inevitably occur. It is worth noting that force field parameters are equivalent for a pair of isomers. Accordingly, if molecular changes are different for the two isomers, they should be related to changes in the liquid crystalline behavior. To specifically address these molecular modifications, it has been shown that reporting the behavior of the different nonbonded energy terms with temperature is a key factor in revealing the actual arrangement inside a mesophase.[18] To characterize specific molecular domains, i.e., inside a layer or between layers, the two nonbonded energy terms, vdW (eq 1) and Coulomb (eq 2), are split into short- and long-range contributions. The short-range (SR) contribution includes interactions between atoms separated by a distance shorter than the cutoff distance, which has been defined as 1.15 nm in the present work. This distance is shorter than half of the shortest cell edge, in agreement with the minimum image convention.[38] Inside this cutoff distance, all vdW interactions are computed using eq 1. Beyond this distance, the so-called long-range (LR) domain, vdW interactions are calculated assuming a unity value for the radial distribution function.[38]

dx.doi.org/10.1021/jp5011605 | J. Phys. Chem. B 2014, 118, 4037−4043

To compute Coulomb interactions, the particle-mesh Ewald (PME) scheme[39] was used based on the Ewald summation method.[22,23] Below the cutoff distance (1.15 nm), interactions are computed in the direct space according to eq 2, thanks to the use of a weight factor. This factor is the complementary error function (erfc) in GROMACS. It makes possible the efficient computation of interactions beyond the cutoff distance, i.e., the LR domain, in the reciprocal space.

Separation of each of the intermolecular energy terms makes available differentiation in molecular arrangement along or between smectic layers. The SR contribution mainly reveals interactions between a mesogen and its first and second neighbors inside a smectic layer, whose separation distance is below 1.15 nm. Interactions between mesogens that are more than two molecules apart belonging to the same smectic layer, and between molecules belonging to different layers, are thus pictured through the LR contribution. Those domains of interactions are schematically displayed in Figure 4 for a SmC

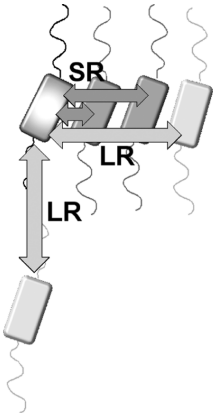

Figure 4. Identification of the molecular contribution to short-range (SR) and long-range (LR) interactions in a SmC arrangement.

arrangement. Analysis of the SR interactions will yield information about lateral arrangement of molecules, i.e., inside a smectic layer. Accordingly, a more negative SR Coulomb interaction between two structural isomers is linked to mesogens that are more packed inside their respective layer. Figure 4 underlines that the situation is not so straightforward for LR interactions. Structural information gained from the study of LR interactions are concerned with both intralayer and interlayer organization. Thus, a simple relationship between LR Coulomb energy and interlayer distance cannot be expected. Nevertheless, all our simulation data show that the isomer with a more negative LR Coulomb interaction is concomitant with a shorter interlayer distance, as compared to its isomeric counterpart. In the Supporting Information, Figure S2 illustrates this observation in the case of C10-Coo-tSC10 and C10-ooC-tSC10. It can thus be argued that longitudinal arrangement is characterized by values of the LR interaction energy. A more negative value is linked to closer longitudinal packing of the molecules for that particular isomer.

Investigation of the behavior of the SR and LR vdW (eq 1) interaction potential energy with respect to the temperature leads to conclusions similar to those resulting from the previous analysis of molecules from the C-series.[18] The graphs are shown in the Supporting Information (Figure S3). Such similarity was expected because the actual difference between the S- and the C-series lies in the distribution of partial charges around the outboard dipole. The vdW potential energy is mainly dominated by the length of the terminal alkyl chains rather than by the direction of the in-core ester or out-board dipole.[18] The two structural isomers (Chart 1) of the S-series are almost indistinguishable based on this interaction.

Behavior of the SR Coulomb interaction potential energies with respect to the temperature for the two mesogens of the S-series with different in-core dipole directions is shown in Figure 5a. For comparison, results for the homologue molecules from

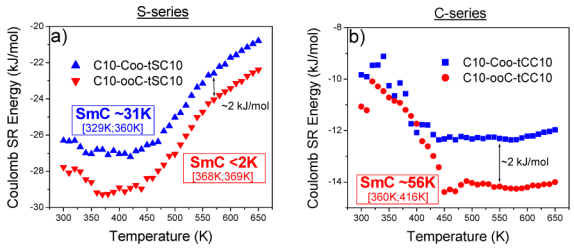

Figure 5. Short-range Coulomb interaction potential energies: (a) S-series and (b) C-series from our previous work.[18] When the SmC phase experimentally exists, its temperature stability range is indicated.

the C-series are displayed in Figure 5b.[18] As previously stated, differences in energy between two structural isomers are mostly discussed because they share the same force field parameters.

For both series at high temperatures, energy associated with the ooC-tX (X = C or S) isomer is around 2 kJ/mol more negative than that for the Coo-tX isomer. The same difference was observed for mesogens from both series with alkyl chain lengths of 6 carbon atoms (Figure S4 in the Supporting Information). This confirms that the energy difference is due to the dipole moment of the ester inside the rigid core. Moreover, the most negative SR Coulomb energy suggests that ooC-tX molecules are more closely packed inside their layers than their isomer (Figure 4). The relation between the values of the SR Coulomb energy and the molecular packing is sketched in Figure 6a. This observation is supported by experiment. The first mesophase of ooC-tS isomer appears 44 K higher than the mesophase of the Coo-tS homologue (Figure 1). Considering comparable change in entropy for both molecules, this indicates that ooC-tS exhibits the largest change in latent enthalpy at the phase transition from the crystal to the mesophase. This

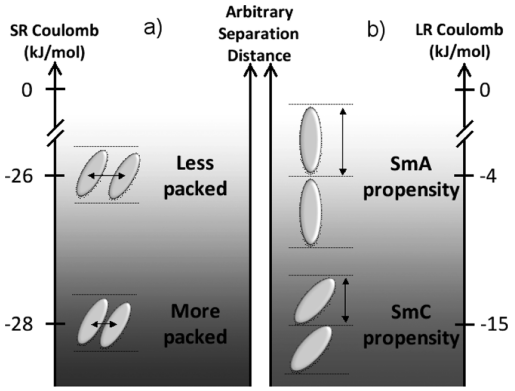

Figure 6. Correlation between simulated Coulomb interactions (310 K) among molecules and experimentally observed molecular arrangements: (a) SR interaction correlated to intralayer packing illustrated with the S-series and (b) LR interaction correlated to interlayer packing illustrated with the C-series. Details in the text.

dx.doi.org/10.1021/jp5011605 | J. Phys. Chem. B 2014, 118, 4037−4043

outcome is consistent with a closer packing of molecules. In the case of the C series, it is also the ooC-tC isomer that shows a transition temperature between the crystal and the mesophase higher than its homologue, a difference of 36 K. It is noteworthy that the closer packing of the ooC-tS molecules leads to the display of a small SmC domain of temperature as compared to the larger domain displayed by the Coo-tS isomer. This observation will be discussed in the light of the other results.

From the previous study on ester series, it was shown that the thermal stability of the SmC phase is governed by the value of the LR Coulomb interaction potential energy.[18] This previous work led to two main conclusions. (i) Among the different energy terms, it is the LR Coulomb interaction that mostly depends on the direction of the ester in the rigid core, which for the C-series is concomitant with the appearance of the SmC phase. (ii) The mesogens displaying the SmC phase in their experimental polymorphism, C10-ooC-tCC10, exhibit the most negative LR Coulomb interaction potential energy. The initial interlayer SmC arrangement (Figure 4) is therefore more favorable for these molecules. Conversely, a less negative LR Coulomb potential energy, as for C10-Coo-tCC10, indicates that molecules belonging to adjacent layers tend to move away from each other, promoting the smectic A (SmA) phase. This statement is supported by the experimental liquid crystalline polymorphism (Figure 1). Conclusions stemming from the analysis of the behavior of the LR Coulombic energy are schematically displayed in Figure 6b.

The LR Coulomb interaction potential energies versus the temperature are shown for mesogens with different in-core dipole directions for the S-series and C-series[18] in panels a and b of Figure 7, respectively. For both series, the ooC-tX isomer

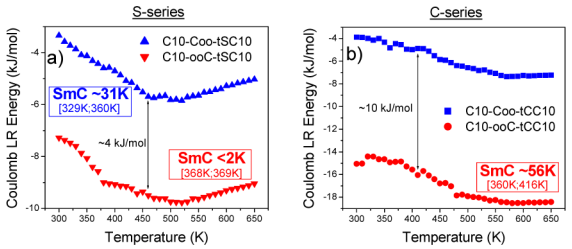

Figure 7. Long-range Coulomb interaction potential energies: (a) S-series and (b) C-series from our previous work.[18] When the SmC phase experimentally exists, its temperature stability range is indicated.

exhibits the most negative LR Coulomb interaction potential energy. However, in the case of the S-series, both molecules exhibit the SmC phase. More precisely, this mesophase occurs on a very small domain of temperature (<2 K for the pure compound, Figure 1) for the ooC-tS isomer, and a relatively broad domain for the Coo-tS isomer (~31 K for the pure compound, Figure 1).

To explain this difference between the two series, the behavior of the SR Coulomb potential energy that reveals arrangement of molecules inside a smectic layer must be taken into account. As has been outlined (Figure 5a), the ooC-tS isomer possesses the lowest SR Coulomb potential energy. Thus, molecules have a tendency to be more packed, reducing the chance to get a mesophase, as evidenced by the high temperature of transition from crystal to the mesophase. Further experiments are requested to confirm this tendency. Binary phase diagrams are of particular interest to disclose the strength of molecular assembly in liquid crystals. More specifically, we consider mixtures between two LC with comparable cohesive energy, one exhibiting the SmC phase in its polymorphism and the other the SmA only. If the SmC phase rapidly vanishes after addition of the smectogen A, it indicates that interactions between molecules within the SmC phase are not significant to still ensure the presence of this mesophase. Conversely, a large range of stability of the SmC phase denotes a strong SmC character. Binary phase diagrams between mesogens from the S-series and the C10-Coo-tCC10 molecule (Figure 8) have thus been prepared. This latter

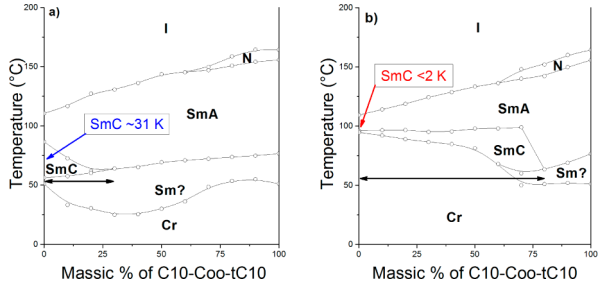

Figure 8. Experimental binary phase diagrams. Binary mixture of C10-Coo-tCC10 with (a) C10-Coo-tSC10 (SmC stability range around 30 K) and (b) C10-ooC-tSC10 (SmC stability range less than 2 K).

molecule from the C-series has been chosen because it does not display the SmC phase and its structure differs little from the molecules of the S-series.

In the binary phase diagram with the mesogen of the S-series possessing the largest SmC temperature domain as a pure compound, i.e., C10-Coo-tSC10, the SmC temperature domain disappears after only 25% weight of C10-Coo-tCC10 (Figure 8a), indicating a weak self-assembly. The related expansion of the SmA phase agrees very well with previous conclusions stemming from studies on the C-series (Figure 6b), where less negative LR Coulomb interaction potential energy (Figure 7a) was concomitant with thermal stability of the SmA.[18] In the binary phase diagram involving C10-ooC-tSC10, for which the SmC domain is small for the pure compound, the temperature domain of this mesophase increases. The occurrence of this mesophase is preserved up to 75% weight of C10-Coo-tCC10 (Figure 8b). It confirms that the ooC-tS molecule that displays the small SmC temperature range (<2 K for the pure compound, Figure 1) has a proficiency for stabilizing the SmC phase that is greater than that of its counterpart, the Coo-tS molecule (SmC range ~30 K for the pure compound, Figure 1). Such a result for the S-series is in perfect agreement with conclusions stemming from previous simulations of the C-series (Figure 6b) because the ooC-tS molecule displays the most negative LR Coulomb interaction potential energy (Figure 7a).

A balance undoubtedly exists between SR and LR interactions to account for the very occurrence of the SmC phase in the polymorphism of a compound. Concerning the S-series, from the liquid crystalline polymorphism of the binary mixtures, it can be seen that the C10-ooC-tSC10 molecule shows a greater proficiency to stabilize the SmC phase (Figure 8b). Computationally, it exhibits a more negative LR Coulomb interaction (Figure 7a), which tends to promote the SmC arrangement over the SmA (Figure 6b), as well as a more negative SR Coulomb energy (Figure 5a) that indicates a closer packing of molecules inside the layer (Figure 6a). Comparison

dx.doi.org/10.1021/jp5011605 | J. Phys. Chem. B 2014, 118, 4037−4043

between experimental and computational outcomes leads to the conclusion that the SR contribution prevails over the entropic contribution. Accordingly, the transition from the crystal to the mesophase appears at higher temperature. To put it another way, interactions that are too strong lead preferentially to the development of crystal over the very existence of the mesophase. In the case of the C10-Coo-tSC10 molecule, SR interactions are not strong enough to make the crystal encroach upon the mesophase, yielding a greater domain of existence for the SmC phase. The same analysis suitably applies to explain the different liquid crystal polymorphism of the C-series molecules. Computationally, C10-ooC-tCC10 exhibits the most negative LR Coulomb interaction (Figure 7b) between the two isomers, which tends to promote the SmC arrangement over the SmA (Figure 6b), as well as a more negative SR Coulomb interaction (Figure 5b). The SR Coulomb values for this series (∼−11 kJ/mol at 310 K, Figure 5b) are clearly weaker than those for the S-series (∼−27 kJ/mol at 310 K, Figure 5a). Accordingly, the fostering of the crystal over the SmC phase is less likely to occur for this series, and a large SmC domain is displayed. In the case of the C10-Coo-tCC10 isomer, the less negative LR Coulomb interaction fosters a large SmA domain.

CONCLUSION

Full-atom molecular simulations supported by experimental characterization have been carried out on two series of isomers. The two series differ from each other by their outboard dipole: a sulfinic and carboxylic ester, defining the S- and C-series, respectively. The main asset in studying isomers in molecular simulation is that they possess the same force field parameters. Differences in averaged properties are then attributed to changes in molecular structural characteristics only. Thermal stability of the SmC phase was specifically studied. Two isomers with different liquid crystalline polymorphisms were selected for each series. Moreover, we built a new model where molecular dynamics simulation are run from an initial SmC arrangement of the molecules. As the temperature is increased, molecules adjust themselves to specifically account for neighborhood interactions. Any changes in this imposed initial self-assembly is thus captured by values of the nonbond energy. More specifically, the Coulomb potential energy is split into two terms that allow for a distinction between lateral and longitudinal molecular organization. Results stemming from the study of S-series isomers have then been supported by published conclusions on the C-series. To strengthen these results, experimental binary phase diagrams have been investigated. Mesogens that possess a greater propensity to disclose the SmC phase in their experimental polymorphism exhibit the most negative long-range Coulomb interaction potential energy. Nevertheless, the actual display of the SmC mesophase is a balance between short-range interactions, which reveal arrangement of molecules within a smectic layer, and long-range interactions, which disclose organization of layers. Our new approach thus results in new understanding of the thermal stability of the SmC phase from the MD viewpoint with direct experimental correlations.

Rules governing the aforementioned balance have been identified. Could they be quantified? For instance, does a universal ratio between Coulomb long-range and short-range energy values that leads to the very existence of the SmC phase exist? Comparison can actually be readily made between structural isomers, but comparison between nonisomers is still problematic because of the use of different force field parameters. To tackle this problem, studies on new families of mesogens should confirm our results and widen the applicability of our model to guide the design of liquid crystal materials for ferroelectric or nonlinear optical applications.

ASSOCIATED CONTENT

Supporting Information

Radial distribution function at 650 K; values of the missing parameters from the original OPLS force field, involving the sulfinic ester; values of one-third of the simulation cell dimension parallel to the three initial smectic C layers and LR Coulomb values, reported against the temperature; vdW interaction potential energies for the S-series, reported versus the temperature; short-range Coulomb interaction potential energies for the homologue molecules with alkyl chains containing six carbon atoms, reported versus the temperature. This material is available free of charge via the Internet at http://pubs.acs.org.

AUTHOR INFORMATION

Corresponding Author

*Département de Chimie, Université de Sherbrooke, 2500, Boulevard de l'Université, Sherbrooke (Québec), J1K 2R1, Canada. Tel.: +1-819-821-7650. Fax: +1-819-821-8017. E-mail: armand.soldera@usherbrooke.ca.

Notes

The authors declare no competing financial interest.

ACKNOWLEDGMENTS

The computational resources were provided by Calcul Québec and Compute Canada. This work was supported by the Université de Sherbrooke, the Fonds Québécois de la Recherche sur la Nature et les Technologies (FRQNT), and the Natural Sciences and Engineering Research Council of Canada (NSERC).

ABBREVIATIONS

LC, liquid crystal; SmC, smectic C; SmA, smectic A; MD, molecular dynamics; vdW, van der Waals; SR, short-range; LR, long-range; OPLS, optimized potential for liquid simulations

REFERENCES

(1) Wulf, A. Steric Model for the Smectic-C Phase. *Phys. Rev. A* **1975**, *11*, 365−375.

(2) McMillan, W. L. Simple Molecular Theory of the Smectic *C* Phase. *Phys. Rev. A* **1973**, *8*, 1921−1929.

(3) Gray, G. W. *Molecular Structure and the Properties of Liquid Crystals*. Academic Press: London, 1962; p 314.

(4) Soldera, A.; Nicoud, J. F.; Skoulios, A.; Galerne, Y.; Guillon, D. Ferroelectric Liquid-Crystals with a Tolane Rigid Core and an Optically-Active Alkyl Sulfinate Group: Synthesis, Characterization, Molecular Modeling, and Stereochemical Investigations. *Chem. Mater.* **1994**, *6* (5), 625−632.

(5) Perreault, F.; Champagne, B.; Soldera, A. Theoretical Design of Sulfinate-Based Ferroelectric Liquid Crystals Displaying Second-Order Nonlinear Optical Properties. *Chem. Phys. Lett.* **2007**, *440* (1−3), 116−120.

(6) Soldera, A.; Theberge, R. Towards a New Class of Ferroelectric Liquid Crystal Molecules for Nonlinear Optical Applications. *Liq. Cryst.* **2003**, *30* (10), 1251−1254.

(7) Champagne, B.; Guthmuller, J.; Perreault, F.; Soldera, A. Theoretical Design of the Molecular Structure of Bent-Core Mesogens with Large Second-Order Nonlinear Optical Properties. *J. Phys. Chem. C* **2012**, *116*, 7552−7560.

(8) Gray, G. W.; Goodby, J. W. *Smectic Liquid Crystals: Textures and Structures*. Leonard Hill: Glasgow, 1984.
(9) Wilson, M. R. Molecular Simulation of Liquid Crystals: Progress Towards a Better Understanding of Bulk Structure and the Prediction of Material Properties. *Chem. Soc. Rev.* **2007**, *36*, 1881−1888.
(10) Govind, A. S.; Madhusudana, N. V. A Molecular Theory of Smectic C Liquid Crystals Made of Rod-Like Molecules. *Eur. Phys. J. E* **2002**, *9*, 107−126.
(11) Gennes, P.-G. d.; Prost, J. *The Physics of Liquid Crystals*, 2nd ed.; Clarendon Press: Oxford, 1993; pp *xvi*, 597.
(12) Nguyen, T.-S.; Geng, J.; Selinger, R. L. B.; Selinger, J. V. Nematic Order on a Deformable Vesicle: Theory and Simulation. *Soft Matter* **2013**, *9*, 8314.
(13) Liao, M.-L.; Ju, S.-P.; Chang, C.-Y.; Huang, W.-L. Size and Chain Length Effects on Structural Behaviors of Biphenylcyclohexane-Based Liquid Crystal Nanoclusters by a Coarse-Grained Model. *J. Mol. Model.* **2012**, *18*, 2321−2331.
(14) Zhang, J.; Su, J.; Ma, Y.; Guo, H. Coarse-Grained Molecular Dynamics Simulations of the Phase Behavior of the 4-Cyano-4′-pentylbiphenyl Liquid Crystal System. *J. Phys. Chem. B* **2012**, *116*, 2075−2089.
(15) Berardi, R.; Muccioli, L.; Zannoni, C. Can Nematic Transitions Be Predicted by Atomistic Simulations? A Computational Study of the Odd-Even Effect. *ChemPhysChem* **2004**, *5*, 104−111.
(16) Metatla, N.; Soldera, A. The Vogel−Fulcher−Tamman Equation Investigated by Atomistic Simulation with Regard to the Adam−Gibbs Model. *Macromolecules* **2007**, *40* (26), 9680−9685.
(17) Soldera, A. Atomistic Simulations of Vinyl Polymers. *Mol. Simul.* **2012**, *38*, 762−771.
(18) Vadnais, R.; Beaudoin, M. A.; Soldera, A. Study of the Influence of Ester Orientation on the Thermal Stability of the Smectic C Phase: Simulation Investigation. *J. Chem. Phys.* **2008**, *129* (16), 164908.
(19) Humphrey, W.; Dalke, A.; Schulten, K. VMD - Visual Molecular Dynamics. *J. Mol. Graphics* **1996**, *14*, 33−38.
(20) Jorgensen, W. L.; Maxwell, D. S.; Tirado-Rives, J. Development and Testing of the OPLS All-Atom Force Field on Conformational Energetics and Properties of Organic Liquids. *J. Am. Chem. Soc.* **1996**, *118*, 11225−11236.
(21) Cramer, C. J. *Essentials of Computational Chemistry: Theories and Models*. 2nd ed.; J. Wiley: Chichester, West Sussex ; Hoboken, NJ, 2004; pp *xx*, 596.
(22) Toukmaji, A. Y.; Board, J. A., Jr. Ewald Summation Techniques in Perspective: A Survey. *Comput. Phys. Commun.* **1996**, *95*, 73−92.
(23) Ewald, P. P. Die Berechnung Optischer und Elektrostatischer Gitterpotentiale. *Ann. Phys. (Berlin, Ger.)* **1921**, *369*, 253−287.
(24) Frisch, M. J.; Trucks, G. W.; Schlegel, H. B.; Scuseria, G. E.; Robb, M. A.; Cheeseman, J. R.; Scalmani, G.; Barone, V.; Mennucci, B.; Petersson, G. A.; et al., *Gaussian 09*, Gaussian, Inc.: Wallingford, CT, 2009.
(25) Jorgensen, W. L.; Tirado-Rives, J. Molecular Modeling of Organic and Biomolecular Systems Using BOSS and MCPRO. *J. Comput. Chem.* **2005**, *26*, 1689−1700.
(26) Bekker, H.; Berendsen, H. J. C.; Dijkstra, E. J.; Achterop, S.; van Drunen, R.; van der Spoel, D.; Sijbers, A.; Keegstra, H.; Reitsma, B.; Renardus, M. K. R., Gromacs: A Parallel Computer for Molecular Dynamics Simulations. In *Proceedings of the 4th International Conference on Physics Computing '92*, Prague, Czechoslovakia, Aug 24−28, 1992; de Groot, R. A.; Nadrchal, J., Eds. World Scientific: Singapore, 1993.
(27) Berendsen, H. J. C.; van der Spoel, D.; van Drunen, R. GROMACS: A Message-Passing Parallel Molecular Dynamics Implementation. *Comput. Phys. Commun.* **1995**, *91*, 43−56.
(28) Lindahl, E.; Hess, B.; van der Spoel, D. GROMACS 3.0: A Package for Molecular Simulation and Trajectory Analysis. *J. Mol. Model.* **2001**, *7*, 306−317.
(29) Van Der Spoel, D.; Lindahl, E.; Hess, B.; Groenhof, G.; Mark, A. E.; Berendsen, H. J. C. GROMACS: Fast, Flexible, and Free. *J. Comput. Chem.* **2005**, *26*, 1701−1718.
(30) Hess, B.; Kutzner, C.; van der Spoel, D.; Lindahl, E. GROMACS 4: Algorithms for Highly Efficient, Load-Balanced, and Scalable Molecular Simulation. *J. Chem. Theory Comput.* **2008**, *4*, 435−447.
(31) Verlet, L. Computer "Experiments" on Classical Fluids. I. Thermodynamical Properties of Lennard-Jones Molecules. *Phys. Rev.* **1967**, *159*, 98−103.
(32) Haile, J. M. *Molecular Dynamics Simulation*. John Wiley & Sons: New York, 1992.
(33) Nosé, S. A Molecular Dynamics Method for Simulations in the Canonical Ensemble. *Mol. Phys.* **1984**, *52*, 255−268.
(34) Hoover, W. G. Canonical Dynamics: Equilibrium Phase-Space Distributions. *Phys. Rev. A* **1985**, *31*, 1695−1697.
(35) Parrinello, M. Polymorphic Transitions in Single Crystals: A New Molecular Dynamics Method. *J. Appl. Phys.* **1981**, *52*, 7182−7190.
(36) Vadnais, R.; Beaudoin, M. A.; Beaudoin, A.; Heinrich, B.; Soldera, A. Study of the Influence of Ester Orientation on the Thermal Stability of the Smectic C Phase: Experimental Investigation. *Liq. Cryst.* **2008**, *35*, 357−364.
(37) Levert, E.; Lacelle, S.; Zysman-Colman, E.; Soldera, A. Influence of Molecular Structure on Phase Transitions in Liquid Crystal Binary Mixtures: The Role of the Orientation of the Central Ester. *J. Mol. Liq.* **2013**, *183*, 59−63.
(38) van Der Spoel, D.; Lindahl, E.; Hess, B.; van Buuren, A. R.; Apol, E.; Meulenhoff, P. J.; Tieleman, D. P.; Sijbers, A. L. T. M.; Feenstra, K. A.; van Drunen, R.; Berendsen, H. J. C.; *GROMACS User Manual Version 4.6.3*, www.gromacs.org, 2013.
(39) Darden, T.; York, D.; Pedersen, L. Particle Mesh Ewald: An $N\cdot\log(N)$ Method for Ewald Sums in Large Systems. *J. Chem. Phys.* **1993**, *98*, 10089−10092.